Prediction of the permeability-reducing effect of cement infiltration into sandy soils

Jinlan Ji and Guisheng Fan

ABSTRACT

Univariate analysis on the permeability-reducing effects of cement infiltration into sandy soil was carried out using a series of experiments on sandy soil infiltrated by adding fine cement grains. The SPSS statistical analysis software was used on these experimental data to construct multivariate prediction models on the permeability-reducing effects of cement infiltration into sandy soils. The results indicate that it is possible to predict permeability-reducing effects using transfer functions. Relatively satisfactory predictions were achieved by inputting the postponed time of water supply, soil dry density, quantity of added cement, water pressure head of cement infiltration, physical clay-silt particle content of soil, and other factors as independent variables. A comparison between the multivariate linear and non-linear models showed that the two models had similar accuracy. The multivariate linear model is relatively simple, and hence can be used to predict permeability-reducing effects. The development of the models has scientific implications for soil modification by altering soil permeability through cement infiltration. It also has practical significance in predictive research on reducing the migration of ground surface pollutants into groundwater.

Key words | cement, infiltrate, permeability-reducing effect, prediction, SPSS

Jinlan Ji
Guisheng Fan (corresponding author)
College of Environmental Science and Engineering,
Taiyuan University of Technology,
Taiyuan,
Shanxi Province 030024,
China
E-mail: *fanguis5507@263.net*

Jinlan Ji
Jincheng Institute of Technology,
Jincheng 048026,
China

INTRODUCTION

During groundwater recharge by infiltration of surface water, pollutants from the ground surface, including sewage, can migrate into the groundwater via soil moisture, leading to groundwater pollution (Page *et al.* 2012). In the long term, temporary garbage disposal sites and river channels or trenches used for the transport of ground surface sewage will inevitably become major sources of groundwater pollution (Bekhit *et al.* 2009). Therefore, researchers and governments of various countries have considered the reduction and management of groundwater pollution by surface sewage to be an important research topic for this century (Zhang *et al.* 2013). The different levels of government in China have explicitly prohibited the use of ditches or ponds without effective leakage prevention measures within the designated protection areas of reserve groundwater sources. However, the ditches, sewage discharge trenches, and temporary garbage disposal sites in some rural towns and most rural villages in China are generally not equipped with effective leakage prevention measures. If these pollutant-carrying areas are located in regions with loose geological formations or cones of groundwater depression, under the effect of water potential gradient, garbage leachate or sewage with high pollutant contents will infiltrate into the groundwater through the upper soil layer, causing irreversible, adverse effects on the groundwater (Juana 2001). The current situation calls for an inexpensive, simple, and user-friendly leakage prevention measure. Walter *et al.* (2000) suggested the placement of artificial capillary barriers, according to the capillary pore characteristics of different soils, to protect sensitive groundwater. The research by Li *et al.* (2012) concluded that the cofferdams of garbage dumps and the clay layer underneath

doi: 10.2166/ws.2016.183

could effectively block pollutants from dredged sediments. The new permeable reactive barriers technology (Wu *et al.* 2016) integrates physical barrier technology with chemical reactions and biological purification technology. The study by Hyung & Young (2013) on cement infiltration into sandy soil discovered that, at a certain effective depth, the infiltration of cement slurry into large pores in the soil matrix could reduce the porosity of the matrix and enhance its permeability-reducing effect.

Fine cement grains can infiltrate into sandy soil and form clusters, thereby blocking large pores of the topsoil and enhancing the permeability-reducing effect of sandy soil (Ji & Fan 2016). On the basis of this, some major factors influencing the permeability-reducing effect due to cement infiltration into sandy soils were investigated and analysed in this study. The SPSS software was used to carry out multiple regression analysis on the experimental data (Kalinski & Yerra 2006) to develop appropriate mathematical prediction models. The models can be used to predict the permeability-reducing effects of cement infiltration into sandy soil matrices under different infiltration conditions. The aim of this research is to reduce the advection of ground surface pollutants into groundwater by controlling the amount of sewage migration, thus contributing to soil modification research and providing scientific evidence for the reduction of groundwater pollution by surface water.

MATERIALS AND METHODS

Test materials

Soil samples were obtained from sandy soils of different river channels, trenches, and temporary garbage disposal sites. The samples were taken at a depth of 0–30 cm, and their sand (20–2,000 μm particle size) content was 72–80%. Sieve analyses indicated that the samples were sandy soils or sandy loam. The cement was ordinary commercial Portland cement (model P·O 42.5, 92% of grain diameter <32 μm). According to the test simulation requirements, water used in the test included manually formulated sewage with sewage effluent from the Fen River, and tap water as a control for comparison.

Test equipment

The test equipment consisted of a set of indoor pressure infiltration devices. Each device consisted of three parts: an infiltration system; a water supply system; and a cement addition system. The infiltration system simulated the infiltration of soil water, which consisted mainly of an infiltration column that was 10 cm in diameter and 100 cm in height. The main body of the water supply system was a Markov tube, which provided a constant water head for the infiltration column and measured the water volume accurately. The function of the cement addition system was to distribute cement grains evenly in the cement slurry, so that the cement would infiltrate into the soil sample matrix with the infiltration water at a set water head.

Test methods

Univariate tests were used as the analytical method, and important factors that might influence cement infiltration were selected for analysis. In this study, the permeability-reducing effect (R_i in %) was used to express the effect of cement infiltration. Here, R_i is defined as the percentage decrease between the average infiltration rate of the test sample and that of the control sample (CK) during a relatively stable infiltration stage, that is, the infiltration reduction rate at relatively stable infiltration rates. Based on the test results, this paper mainly discusses the dominant factors, such as soil texture, soil structure (Kalinski & Yerra 2006), quantity of added cement (*QAC*), postponed time of water supply (*PT*) (Ji & Fan 2015), water pressure head of cement infiltration (*WPH*) (Sun *et al.* 2014), and water quality for infiltration. A CK was also used in the analysis of each factor, and at least four test levels were set. When the cement slurry infiltrated into the soil sample column during the experiments, an identical amount of tap water was added to the CK to ensure that both samples had the same initial moisture content.

DEVELOPMENT OF THE PREDICTION MODELS

In this study, R_i was designated as the prediction variable (dependent variable). Based on the experimental results, a multiple linear regression statistical model was developed to simulate the interaction between R_i and its dominant factors, i.e., predictor variables. According to the functional relationship between R_i and each factor, a non-linear model between the two was developed. Following this process, an easy-to-use model with relatively high prediction accuracy was selected as the permeability-reducing effect prediction model, by comparing the prediction results with the actual observations. In principle, a higher number of independent variables implies a greater regression sum of squares, and a smaller residual mean value, thus giving better prediction results. However, the difficulty of prediction procedures increases with the number of independent variables, and may lead to interactions between the independent variables. Moreover, some independent variables may have insignificant effects on the dependent variable, but may affect the prediction results instead (Fan *et al.* 2013). In these situations, principal component analysis is needed (Azid *et al.* 2014). Using linear combinations, the original variables are integrated into several principal components, and the large number of original variables are replaced by a reduced number of components (Hajiaghaei *et al.* 2014). After this process, each factor was subjected to regression analysis to develop the simulation equations. The effect of less significant factors was included in the constant terms, and the reliability of the simulation model was determined by an *F*-test.

Mathematical relationship between R_i and each factor

Soil texture

Soil texture refers to the combination of mineral particles of various diameters in soil, which defines the proportion of macro-pores and porosity of the soil. If the soil pores are greater than the effective particle size of the cement grains, the cement slurry can infiltrate into the surface soil under the soil water potential gradient (Martin *et al.* 2014). In the analysis, soil texture was expressed by clay content, silt content, and sand content. To simplify the independent variables, we reduced the soil texture characterisation indices to two, the content of clay (*CC*) and content of clay-silt (*CCS*). In principle, when cement grains infiltrate into soil, the R_i will be greater when there is more effective infiltration of cement particles. In this experiment, more than 90% of the cement particle sizes were concentrated at 3–32 μm, which was similar to the particle size of clay and silt (particle size ≤20 μm) in the soil matrix. As the sand content in the soil increases, the amount of clay and silt decreases, leading to an increase in the number of macro-pores and porosity of the soil matrix. As the resistance to cement infiltration diminishes, in principle, more cement can infiltrate into the soil, thereby increasing its permeability-reducing effect. According to the simulation of the test data, under the fixed infiltration conditions of *QAC* of 1 kg/m^2; *WPH* of 100 cm; soil dry density (*DD*) of 1.4 g/cm^3; and *PT* of 12 h; the R_i and *CCS* showed a positively correlated exponential function, as $R_i = e^{(\alpha+\beta\times \mathrm{CCS}+\gamma\times CCS^2)}$ ($R^2 = 0.9853$, where α, β and γ are the model parameters; and have similar meanings in the following functions).

Soil structure

Soil structure reflects how loose or compact the soil is. The lower the soil *DD*, the looser the soil structure, which leads to a greater number of macro-pores and water-conducting pores for the movement of soil moisture. Thus, cement can infiltrate into the matrix at a higher rate and to a greater depth, leading to a greater degree of effective cement infiltration, and a more significant decrease in hydraulic conductivity. Soil structure is represented by soil *DD*, and is given in units of g/cm^3. The infiltration was done under conditions of *WPH* of 100 cm; *PT* of 12 h; soil *DD*s of 1.3, 1.4, 1.5, and 1.6 g/cm^3; and *QAC*s of 1 kg/m^2 and 3 kg/m^2. The simulation of experimental data shows a negatively correlated exponential function as $R_i = e^{(\alpha+\beta\times \mathrm{DD}+\gamma\times \mathrm{DD}^2)}$ ($R^2_{1\mathrm{kg/m^2 cement}} = 0.9629$, $R^2_{3\mathrm{kg/m^2 cement}} = 0.9682$).

Postponed time of water supply

PT is the time interval between the end of cement infiltration and the beginning of water supply, and is given in units of h. With an increase in *PT*, the cement grains infiltrating into the soil, the surrounding colloidal soil grains, and the cement grains covering the soil surface had sufficient time to cluster and harden, to form a dense structure, and to enhance the permeability-reducing effect. Figure 1 shows the relationship between the R_i and *PT*s (3, 6, 12, 24, and 48 h) for different soils, under the fixed conditions of *QAC* of 1 kg/m^2; *WPH* of 100 cm; and soil *DD* of 1.4 g/cm^3. The same trends were observed for three different soils.

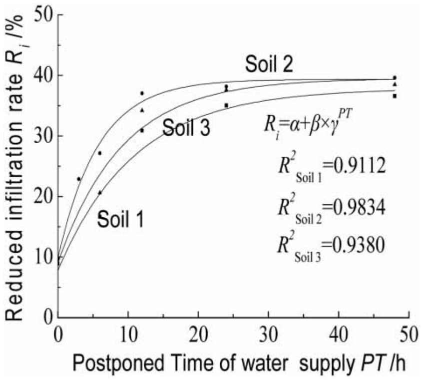

Figure 1 | Relationship between infiltration-reducing effect and postponed time of water supply.

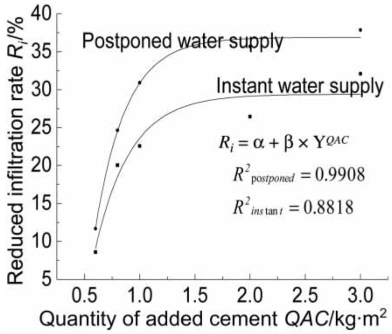

Figure 2 | Permeability-reducing effects of different quantities of cement addition.

Quantity of added cement

QAC is the quantity of cement added to the infiltration system per unit area, and is given in units of kg/m^2. The *QAC* influences the permeability-reducing effect. Firstly, in the initial stage of cement infiltration, due to the high concentration of cement slurry, the test samples with higher *QAC*s showed an infiltration quantity slightly higher than those with lower *QAC*s within the same short period. This higher *QAC* led to higher physical filling and hydration agglomeration, thus causing a difference in the permeability-reducing effect. Secondly, apart from the cement infiltrating into the soil, excess cement particles also accumulate and form a hardened layer on top of the sandy soil, modifying the structure of the surface control layer, and thus increasing its permeability-reducing effect. However, this experiment demonstrated a limited contribution of *QAC* to the permeability-reducing effect. The fixed infiltration conditions were *WPH* of 100 cm; and soil *DD* of 1.4 g/cm^3. *QAC*s of 0.6, 0.8, 1.0, 2.0, and 3.0 kg/m^2 were selected. Figure 2 shows the relationship between infiltration reduction rate and *QACs* under instant water supply and a *PT* of 12 h. Under both conditions, the two variables showed a positively correlated exponential relationship.

Water pressure head of cement infiltration

WPH is the distance between the cement-adding device and the surface soil, and is given in units of cm. The fixed infiltration conditions were *QAC* of 1 kg/m^2; soil *DD* of 1.4 g/cm^3; and a *PT* of 12 h. The *WPH*s of 60, 90, 100, and 120 cm were selected. As indicated by the trend of the test data, with an increase in *WPH*, the potential gradient at the infiltration interface increased, as did the capacity and number of cement grains to infiltrate into the soil, thereby strengthening the permeability-reducing effect. The relationship between the R_i and the *WPH* can be simulated by an exponential function as $R_i = e^{(\alpha+\beta\times WPH+\gamma\times WPH^2)}$ ($R^2 = 0.9423$).

Water quality for infiltration

In this study, this variable was represented mainly by total dissolved solids (*TDS*) and total suspended solids (*SS*), both of which hinder the kinematic viscosity of water, and are given in units of mg/L. During sewage infiltration, because the concentrations of *TDS* and *SS* in sewage are relatively high, the physical viscosity of the fluid body increases (Sun *et al.* 2009), causing an increased flow resistance for the fluid body in soil pores and a decreased infiltration capacity. Furthermore, the *SS* were gradually trapped in the soil during infiltration, thus blocking the soil pores and hindering water infiltration. Some *SS* were deposited on the soil surface, causing resistance to water infiltration, which increased further with longer infiltration times (Martin *et al.* 2014). This reduced the infiltration capacity of the soils for sewage infiltration. Because comparison of the permeability-reducing effect of tap water infiltration and sewage infiltration only were considered in this experiment, and no univariate analysis was carried out on water quality variation, non-linear function modelling was not performed.

Other factors

Other less significant factors, such as the groundwater table and the initial moisture content of soil, were not considered as independent variables in the model, but were included in the constant terms.

In summary, the dependent variable of the model is R_i, and the independent variables are *CC, CCS, DD, QAC, WPH, PT, TDS*, and *SS*, for a total of eight.

Structures of the prediction models

Multiple linear regression model

$$R_i = \alpha_0 + \alpha_1 x_1 + \alpha_2 x_2 + \ldots\ldots + \alpha_k x_n \tag{1}$$

where R_i is the dependent variable; α_0 is the regression constant; α_k ($k = 1, 2, 3, \ldots, n$) is the regression coefficient; and x_n is the n^{th} factor (*PT, DD, WPH, QAC, SS, TDS, CC*, or *CCS*).

Multiple non-linear regression model

The relationships between the permeability-reducing effect and dominant factors can be simulated by exponential functions. To construct a non-linear function model, the logarithm of the dependent variable was taken, where there is a linear relationship between $\mathrm{Ln}R_i$ and each factor of influence, $\mathrm{Ln}R_i = \epsilon + \beta x_1 + \gamma x_2 + \ldots$ (where ε is the error term of each factor, β, γ is the regression coefficient; and x_n is the independent variable such as *WPH*, *WPH*^{2}, etc.). To simplify the equations, the error terms of all factors are contained in the regression constant β_0, and the other terms are accumulated. The equations were simplified to construct a non-linear mathematical model with $\mathrm{Ln}R_i$ and the independent variables.

$$Y = \mathrm{Ln}R_i = \beta_0 + \beta_1 x_1 + \beta_2 x_2 + \ldots\ldots + \beta_\kappa x_n \tag{2}$$

where Y is the log value of the relatively stable infiltration reduction rate; β_0 is the regression constant; β_k ($k = 1, 2, 3, \ldots, n$) is the regression coefficient; and x_n is the n^{th} factor (*PT, DD, DD*^{2}, *WPH, WPH*^{2}, *QAC*, Ln*SS, CCS*, or *CCS*^{2}).

During SPSS regression, when an independent variable has a significant effect on the dependent variable, it is first included in the stepwise regression. When an independent variable does not have a significant contribution to the total regression equation of the dependent variable, i.e., has a *t*-value of less than the value of $t_{0.05/2}$ in a one-tailed *t*-test, it is eliminated. Thus, the system selects the most relevant variables automatically and constructs the 'optimal' regression equation based on these independent variables.

The *t*-test of independent variables

In the regression process of the linear model, SPSS performed eight steps, and the coefficients of the regression equation are given in Table 1. As shown in Table 1, the six factors of *PT, DD, WPH, QAC, SS*, and *CCS* were included in the linear regression equation, and their *t*-values all exceeded $t_{0.05/2}$ (2.009). In the column of significance analysis, all of the Sig. values were lower than 0.05, indicating that the significance levels evaluated by the *t*-test were relatively

Table 1 | Coefficients of stepwise regression equations of the linear model

Linear model (Dependent variable R_i)	Unstandardized coefficients B	Unstandardized coefficients Std. Err.	Standardized coefficient Beta	*t*	Sig.	Collinearity statistics Tolerance	Collinearity statistics VIF
Step 8							
(Constant)	114.859	23.607		4.865	0.000		
PT	0.673	0.080	0.680	8.445	0.000	0.915	1.093
DD	−77.908	16.053	−0.381	−4.853	0.000	0.964	1.038
WPH	0.199	0.052	0.294	3.794	0.000	0.990	1.010
QAC	3.428	1.116	0.252	3.071	0.004	0.883	1.132
SS	−0.178	0.071	−0.197	−2.497	0.016	0.956	1.046
CCS	−0.504	0.130	−0.305	−3.866	0.000	0.956	1.046

high. In collinearity diagnostics, all of the variance inflation factor (VIF) values were less than 5, suggesting that there was no linear correlation between any two residual independent variables. Therefore, these factors could be applied in prediction simulation. The independent variables *TDS* and *CC* were eliminated because of their lower *t*-values.

Using the same method, in the *t*-test of the independent variables in the non-linear model, SPSS performed stepwise regression five times. The software examined nine independent variables in the non-linear model. PT, DD^2, WPH^2, QAC, and CCS^2 were eventually retained in the regression, whereas *DD, WPH,* Ln*SS,* and *CCS* were eliminated.

Prediction models and *F*-test

Prediction models

After substituting the unstandardized coefficients from Table 1 into the multiple regression model, the linear prediction model for infiltration reduction is:

$$R_i = 114.859 + 0.673PT - 77.908DD + 0.199WPH + 3.428QAC - 0.178SS - 0.504CCS \quad (3)$$

The coefficient of each independent variable in model II is listed in Table 2.

The non-linear equation for the dependent variable Y is:

$$\mathrm{Ln}R_i = Y = 6.012 + 0.032PT - 1.980DD^2 - 0.001CCS^2 + 0.225QAC + 6.125 \times 10^{-5}WPH^2 \quad (4)$$

Table 2 | Coefficients of stepwise regression equations of the non-linear model

Step 5	(Constant)	*PT*	DD^2	CCS^2	*QAC*	WPH^2
	6.012	0.032	−1.980	−0.001	0.225	6.125×10^{-5}

Dependent variable: $Y = \mathrm{Ln}R_i$.

Therefore, the non-linear prediction model for infiltration reduction is:

$$R_i = e^Y = e^{6.012+0.032PT-1.980DD^2-0.001CCS^2+0.225QAC+6.125\times10^{-5}WPH^2} \quad (5)$$

F-test of regression models

The *t*-test evaluates the significance of independent variables in equations, whereas the *F*-test is an evaluation of the overall significance of the entire regression equation (Hajiaghaei *et al.* 2014). As shown in Table 3, the adjusted R^2 for the two models are 0.709 and 0.768, indicating relatively high goodness of fit. The analysis on the model prediction results demonstrates that, apart from individual data, the prediction of the linear model for the overall experiment was relatively good. The average prediction error was 6.141%. The *F*-value was much greater than $F_{0.05}$, indicating a significant regression equation. The average prediction error for the non-linear model was 0.283%. The *F*-value for the model was much greater than $F_{0.05}$. Nevertheless, the prediction error was about LnR_i, which when converted to R_i, had a prediction error of 5.863%, again indicating a significant regression equation. These data demonstrate that it is feasible to use these two models to predict the permeability-reducing effects due to cement infiltration into sandy soil.

COMPARISON OF THE PREDICTIONS

In experiments on the permeability-reducing effect performed on four kinds of sandy soil samples, the two models described above were used to predict the reduced

Table 3 | Model summary

Model	*R*	R^2	Adjusted R^2	Std. error of the estimate (%)	*F*	$F_{0.05}$	Sig.
Linear	0.859	0.709	0.703	6.141	20.714	2.290	0.0001
Non-linear	0.876	0.768	0.742	0.283	29.745	2.404	0.0001

Table 4 | Prediction examples of the two models

Soils	(*DD*) g/cm^3	(*WPH*) Cm	(*QAC*) kg/m^2	(*PT*) h	Measured value %	Predicted value Model I %	Predicted value Model II %	Error Model I %	Error Model II %
Soil 1	1.3	100	1	0	22.57	22.78	20.94	0.94	7.22
Soil 1	1.3	100	2	0	26.44	26.21	26.24	0.87	0.77
Soil 2	1.4	100	1	12	37.01	35.03	33.79	5.34	8.70
Soil 2	1.4	100	1	24	38.14	35.11	33.33	7.94	12.60
Soil 3	1.3	100	3	0	32.07	29.64	32.87	7.58	2.49
Soil 3	1.4	100	3	0	19.25	20.70	20.35	7.53	5.71
Soil 4	1.4	60	3	12	22.32	24.25	22.00	8.63	1.42
Soil 4	1.4	120	3	12	42.33	39.16	42.64	7.48	0.73

infiltration rates under specific infiltration conditions. The prediction results are listed in Table 4.

CONCLUSIONS

(1) It is possible to apply the multiple linear and non-linear regression models to predict the permeability-reducing effect due to cement infiltration into sandy soils.
(2) The prediction errors of the permeability-reducing effect by the multiple linear and non-linear regression models were 6.141% and 5.863%, respectively. The non-linear model had a slightly higher prediction accuracy, but the computational workload was heavier. The linear prediction model was simpler and can be applied in preliminary projects relying on the prediction of permeability-reducing effect.
(3) Many factors affect the permeability-reducing effect of cement infiltrating into the soil matrix. By elimination of independent variables, it was found that the *PT*, soil *DD*, *WPH*, and *QAC* were significantly correlated with the permeability-reducing effect. The *SS* content in infiltrating water and the content of clay-silt in the sandy soil also influence the permeability-reducing effect. These factors can be used as input variables for a linear prediction model to predict the permeability-reducing effects due to cement infiltration into sandy soils.
(4) The simulations of the prediction models are based solely on the experimental data collected in this study. The sample size was relatively small, and the multiple non-linear regression model developed was known as a 'black-box model', with relatively low prediction accuracy. Further research on prediction methodology and its theoretical basis is required to attain higher prediction accuracy.

ACKNOWLEDGEMENTS

We offer our sincere thanks for the support of Shanxi Province Science and Technology Development Project under Grant No. 20150313002-2, Shanxi River Management and Protection Services Program under Grant No. Sci. 2012-1, and Jincheng City Science and Technology Development Project under Grant No. 201202238.

REFERENCES

Azid, A., Juahir, H., Toriman, M. E., Kamarudin, M. K. A., Saudi, A. S. M., Hasnam, C. N. C., Aziz, N. A. A., Azaman, F., Latif, M. T., Zainuddin, S. F. M., Osman, M. R. & Yamin, M. 2014 Prediction of the level of air pollution using principal component analysis and artificial neural network techniques: a case study in Malaysia. *Water Air & Soil Pollution* **225** (8), 1–14. DOI:10.1007/s11270-014-2063-1.

Bekhit, H. M., El-Kordy, M. A. & Hassan, A. E. 2009 Contaminant transport in groundwater in the presence of colloids and bacteria: model development and verification. *Journal of*

Contaminant Hydrology **108** (3–4), 152–167. DOI:10.1016/j.jconhyd.2009.07.003.

Fan, G. S., Han, Y. H. & Ma, D. N. 2013 Computer forecasting of the soil water infiltration parameters in seasonal freezing and thawing periods. *Mathematical and Computer Modelling* **58** (3–4), 725–730. DOI: 10.1016/j. mcm.2011.10.031.

Hajiaghaei, A., Rashidi, M., Sadeghi, M. A., Gholami, M. & Jaberinasab, B. 2014 Prediction of soil infiltration rate based on silt and clay content of soil. *American-Eurasian Journal of Agricultural & Environmental Sciences.* **14** (8), 702–706. DOI: 10.5829/idosi.aejaes.2014.14.08.12394.

Hyung, K. P. & Young, C. C. 2013 Prediction of cement infiltration depth in coarse-grained soil. *KSCE Journal of Civil Engineering* **17** (5), 886–894. DOI: 10.1007/s12205-013-0288-y.

Ji, J. L. & Fan, G. S. 2015 Impact of postponed water feeding time on the infiltration-reducing effect of cement into alluvial soils. *Fresenius Environmental Bulletin* **24** (11a), 3766–3773.

Ji, J. L. & Fan, G. S. 2016 Analysis of the main factors influencing the permeability-reducing effect of cement infiltration in a river sediment matrix. *KSCE Journal of Civil Engineering* 1–7. DOI: 10.1007/s12205-016-0599-x.

Juana, P. 2001 Porosity, dispersivity and contaminant transport in groundwater. *Journal of Geoscientific Research In Northeast Asia* **4** (2), 192–199.

Kalinski, M. E. & Yerra, P. K. 2006 Hydraulic conductivity of compacted cement-stabilized fly ash. *Fuel* **85** (16), 2330–2336. DOI:10.1016/j.fuel.2006.04.030.

Li, T., Zhang, Z. H. & Tang, B. R. 2012 Experimental study of retardant effect of clay barriers on contaminants in a confined disposal facility for dredged sediments from Taihu Lake. *Rock and Soil Mechanics* **33** (4), 993–998.

Martin III, W. D., Kaye, N. B. & Putman, B. J. 2014 Effects of aggregate masking on soil infiltration under an aggregate bed. *Journal of Irrigation and Drainage Engineering* **141** (9), 879–884. DOI: 10.1061/(ASCE)IR.1943-4774.0000879.

Page, R. M., Scheidler, S., Polat, E., Svoboda, P. & Huggenberger, P. 2012 Faecal indicator bacteria: groundwater dynamics and transport following precipitation and river water infiltration. *Water Air & Soil Pollution* **223** (5), 2771–2782. DOI: 10.1007/s11270-011-1065-5.

Sun, C. X., Wu, F. Q., Wang, J. & Liu, Q. X. 2009 Experimental studies on muddy water infiltration with different concentration. *Bulletin of Soil and Water Conservation* **29** (8), 57–60.

Sun, Y. X., Fan, G. S. & Ji, J. L. 2014 Study on the effect of effective water head of cement on permeability function of soil matrix. *Yellow River* **36** (12), 85–87.

Walter, M. T., Kim, J. S., Steenhuis, T. S., Parlange, J. Y., Heilig, A., Braddock, R. D., Selker, J. S. & Boll, J. 2000 Funneled flow mechanisms in a sloping layered soil: laboratory investigation. *Water Resources Research* **36** (4), 841–849. DOI: 10.1029/1999WR900328.

Wu, P. Y., Ji, D. F., Su, J., Sun, Y. Y., Cui, C. F., Liang, Y. H., Dang, Q. L. & Tang, J. 2016 Research progress of permeable reactive barrier in the remediation of nitrate pollution in groundwater. *Journal of Environmental Engineering Technology* **6** (3), 245–251. DOI: 10.3969/j.issn.1674-991X.2016.03.037.

Zhang, Y., Liu, C. L., Lv, D. Y. & Wang, Z. L. 2013 Investigation of groundwater pollution prevention strategies. In *Chinese Society for Environmental Sciences. Annual Conference, Kunming, China*. China Environmental Science Press, pp. 3081–3091.

First received 15 August 2016; accepted in revised form 28 October 2016. Available online 15 November 2016